Joint Pathology Center
Veterinary Pathology Services

WEDNESDAY SLIDE CONFERENCE 2026-2027

Conference #3 — 2 September 2026

CASE I:

Signalment:
22 month-old, neutered male, dog, Schnauzer.

History:
The dog was referred to the Veterinary Hospital with a history of weight loss, inappetence, vomiting, and mild diarrhea. Blood samples were collected for total blood cell counts, a biochemical profile, and serological tests to detect anti-*Leishmania* antibodies. Blood samples were collected at admission and weekly while the dog was under medical care. Physical examination demonstrated enlargement of the cervical and popliteal lymph nodes. Clinical examination also revealed abdominal pain,

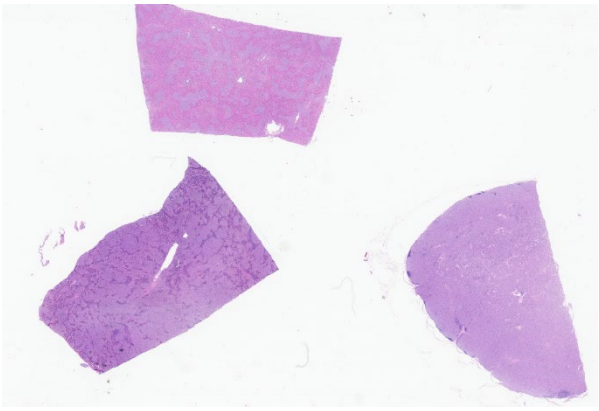

1-1. Liver, spleen, and lymph node, dog. A section of liver, spleen, and lymph node were submitted. Throughout all three sections there is a multifocal to coalescing cellular infiltrate that obscures large regions of the preexisting architecture. (HE, 2x).

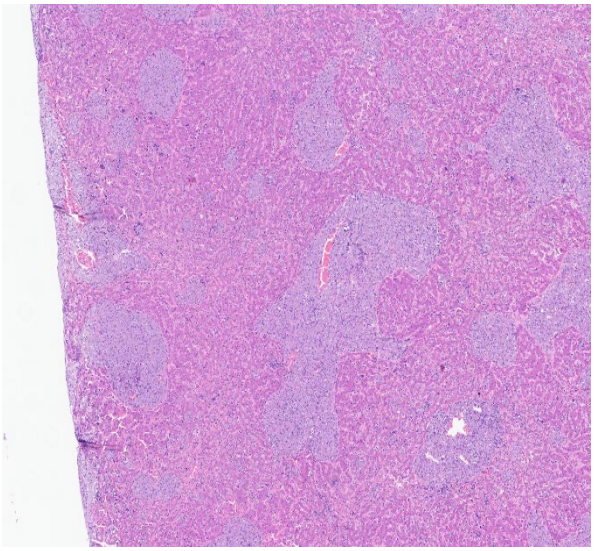

1-2. Liver, dog: The sinusoids are markedly expanded by granulomatous inflammation. (HE, 4x).

hepatomegaly, and splenomegaly. Ultrasonography confirmed splenomegaly and demonstrated intestinal wall thickening. Aspirative cytology evaluation of the spleen and popliteal lymph node was performed. The first blood cell count revealed anemia, thrombocytopenia, and mild monocytosis. Based on the hematology results, erlichiosis was suspected. Based on initial suspicion, doxycycline (5 mg/kg IV bid), maropitant citrate (1 mg/kg sc for 5 d), and fluid (ringer lactate) were prescribed. Therefore, an exploratory laparotomy with splenectomy was performed. The spleen was submitted to histopathology. A re-check five days after the onset of therapy showed no changes on clinical examination. Cytopatho-

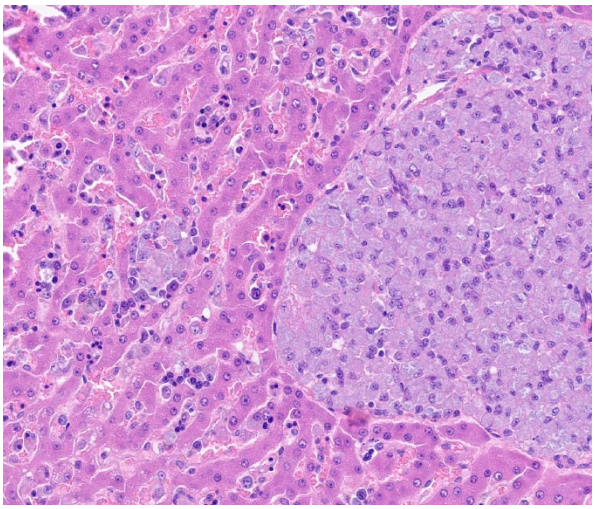

1-3. Liver, dog. Histocytes are epithelioid with abundant amphophilic, granular cytoplasm. (HE, 10x)

logical findings were compatible with histiocytic lymphadenitis and splenitis associated with higher numbers of cell-associated acid-fast bacilli. Then, 20 days after admission, the dog was treated with metronidazol (15 mg/kg, IV, bid, 7 days), amoxicillin and clavulanate (20 mg/kg, IV, bid, 14 days), silymarin (25 mg/kg, vo, sid, 14 dias), ursodeoxycholic acid (15 mg/kg, vo, sid 10 days), ondansetron (0.22 mg/kg, IV, tid, 14 days), and rifampicin (20 mg/kg, vo, tid) used to treat *Mycobacterium* infection. Ten days later, the clinical condition worsened, and the dog presented with regurgitation of food, weakness, and lethargy. The dog was monitored since admission, totaling 30 days, when he died after rapid deterioration of his clinical condition. The owner authorized a cosmetic necropsy. Most organs were collected for histopathology. Samples of spleen and lymph nodes were collected and frozen for molecular analysis.

Gross Pathology:

The spleen (surgically removed) was markedly enlarged, with roughly twice its normal size. The subcapsular surface presented numerous multifocal to coalescing yellow-whitish foci. Approximately 90% of the parenchyma was replaced by multifocal to coalescing prominent, slightly soft, yellow-whitish millimetric areas. Two focally extensive whitish, amorphous, and soft areas measuring approximately 4 cm in diameter were grossly interpreted as caseous necrosis. At necropsy, the dog was emaciated, and the oral and ocular mucosae were white to slightly yellow. All cervical, axillary, popliteal, mediastinal, tracheobronchial, iliac (external and internal), and mesenteric lymph nodes were markedly enlarged, some of which were more than five times their normal size. The capsules of these lymph nodes were tense, and on the cut surface their normal morphologic characteristic were lost, with the cortex and medulla replaced by yellow-whitish solid soft tissue. The ventral portions of the pulmonary lobes (especially on the left side) were dark-red and consolidated, with viscous yellow exudate draining from the bronchial lumen and parenchyma. The liver was markedly enlarged, with rounded edges and a yellowish surface. Filaments and plaques of fibrin were observed on the capsular surface of the right hepatic lobes. On cut surface, multifocal to coalescing slightly prominent yellow-whitish foci were interspersed with red-yellowish parenchyma. Kidneys were pale red, interspersed with several whitish soft foci in the cortex.

Laboratory Results:

Serological tests for *Leishmania*: Indirect immunofluorescent (RIFI) in 1:40 dilution and enzyme-linked immunosorbent assay (ELISA) for IgG were negative.

Clinical pathology:
CBC: 4.79 Hgb, 9.7 Hgb; 28.0 % Hct; 12.912 Seg; 1.603 Mno; 166.000 platelets and metarubricytes, 2.9%.

Biochemical profile: alkaline phosphatase, 552.0 U/L; ALT, 177.35 U/L; AST, 223.73 U/L. Albumin, 1.69 g/dL Popliteal lymph node aspirate biopsy: many macrophages with numerous small vacuoles in the cytoplasm.

Acid-fast (Ziehl-Neelsen) staining of lymph node and spleen aspirates: large numbers of acid-fast bacilli associated with macrophages

Molecular analysis of DNA extracted from spleen and feces:
PCR for *M. bovis, M. tuberculosis* and *M. avium* subsp. resulted negative.

PCR and sequencing identified the bacilli as *Mycobacterium avium* subsp. *avium*.

Histopathologic Description:
Histopathological evaluation of the spleen revealed marked inflammatory reaction replacing the normal architecture. Multifocal to coalescing aggregates of epithelioid macrophages and fewer multinucleated cells compressed and replaced the red and white pulp. The remaining normal red pulp had several nucleated erythroid cells and some megakaryocytes. Lymphocytes and plasma cells were markedly reduced. In addition, a focally extensive area consisted of amorphous eosinophilic material mixed with fibrin and cellular debris.

The lymph node parenchyma was 90 to 95% replaced by macrophages, epithelioid macrophages, and a lower number of multinucleate cells (2-3 nuclei). The remaining parts of the architecture were the subcapsular sinus and the small lymphoid follicles. Inflammatory cells similar to those in the spleen and lymph nodes replaced about 50-60% of the normal liver parenchyma. In the sinusoids of these are as, numerous lymphocytes, several nucleated erythroid cells, and fewer megakaryocytes were present.

The mucosa and submucosa of the small and large intestine were thickened by granulomatous inflammation, composed mostly of epithelioid macrophages and a lower number of multinucleated cells with up to five nuclei. In the small intestine, granulomatous inflammation replaced 90% of the lymphoid follicles (Peyer plaques). Pulmonary lobes showed suppurative bronchopneumonia and fibrinosuppurative pleuritis. In addition, there was an occlusive thrombus in a bronchial artery. Multifocal interstitial and alveolar granulomatous inflammation was also present.

The kidneys had mild multifocal interstitial granulomatous inflammation, similar to that observed in the other organs mentioned above. In addition, moderate membranous glomerulopathy and tubular proteinuria were present.
Ziehl-Neelsen special staining of the spleen, lymph nodes, liver, lungs, kidneys, and intestine showed large amounts of acid-fast bacilli within macrophages and multinucleated cells.

Contributor's Morphologic Diagnoses:
Spleen: marked multifocal to coalescing granulomatous splenitis, lymphoid atrophy, locally extensive lytic necrosis, and moderate extramedullary hematopoiesis.

Lymph nodes: marked diffuse granulomatous lymphadenitis and lymphoid atrophy.

Liver: marked multifocal to coalescing granulomatous hepatitis and moderate extramedullary hematopoiesis.

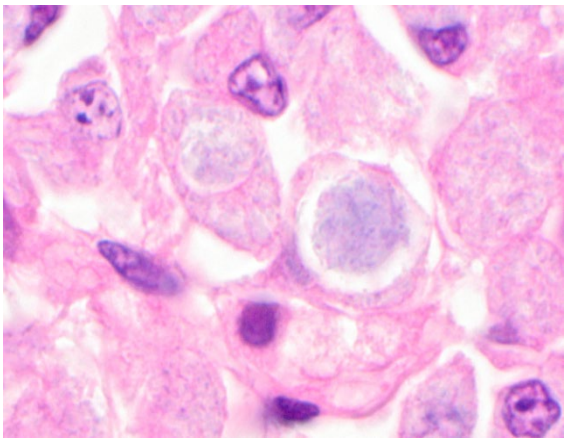

1-4. Liver, dog. Macrophage cytoplasm contains abundant 2 µm basophilic rods. (HE, 100x)

Not submitted tissues:
Small and large intestine (mucosa and submucosa): moderate multifocal to coalescing circumferential granulomatous enteritis and lymphoid atrophy in the gut-associated lymphoid tissue.

Lungs: marked acute suppurative broncopneumonia, and mild multifocal granulomatous pneumonia.

Kidneys: mild multifocal granulomatous nephritis and moderate membranous glomerulopathy associated with tubular proteinuria.

Contributor's Comment:
Gross and histopathological findings associated with acid-fast positive stain were compatible with disseminated mycobacteriosis. The large numbers of intracellular bacilli are more suggestive of mycobacteriosis caused by M. avium. Molecular analysis, including sequencing, confirmed M. avium subsp. avium infection in this dog. The three most common species of Mycobacterium, namely M. tuberculosis (human), M. bovis (cattle), and M. avium (avian species), affect their preferential hosts more often. Still, cross-infections may occur involving several other host species. M. bovis and M. tuberculosis cause tuberculosis characterized by disseminated or localized infections in the lungs or in the gastrointestinal tract. M. avium, one of the species of the M. avium-intracellulare complex (MAC), can cause mycobacteriosis or atypical mycobacterium[4]. The avium species includes 4 subspecies, i.e., M. avium subsp. avium, M. avium subsp. hominissuis, M. avium subsp. silvaticum, and M. avium subsp. paratuberculosis[2, 16]. M. avium subsp. avium infection is common in domestic[11], wild[8,] and exotic captive birds [5], but it is rare in mammals[1]. M. genavense is another common cause of mycobateriosis in birds[12]. In dogs, disseminated mycobacteriosis has also been caused by M. avium subspecies avium[7,1] and M. avium subspecies hominis[9,3]. Disseminated canine tuberculosis caused by M. tuberculosis infection has also been reported[13].

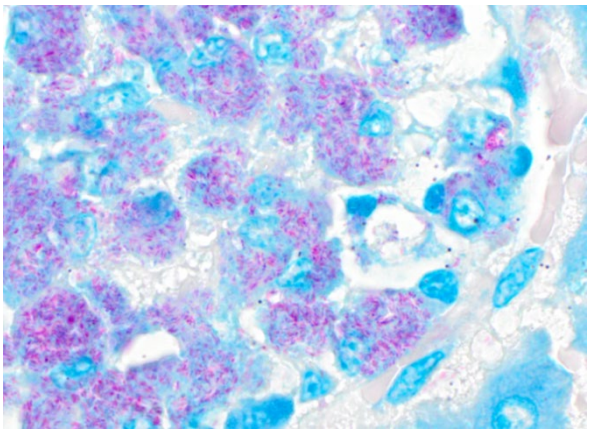

1-5. Liver, dog. Acid fast, 2 um rods markedly expand the cytoplasm of almost all histiocytes throughout regions of granulomatous inflammation. (Ziel-Neeson, 100x)

Lesions produced by M. avium infection are more proliferative and consist of diffuse infiltration of macrophages, epithelioid cells, and multinucleate cells, accompanied by numerous bacilli and extensive fibroplasia. Dogs and cats usually present lesions as granulation tissue[4]. The disseminated infection in this dog was characterized by diffuse granulomatous inflammation (predominantly macrophages and epithelioid cells, with occasional giant cells) with numerous bacilli, similar to M. avium infection in birds. Caseous necrosis was present only in two locally extensive areas in the spleen. Similar findings caused by M. avium were described in dogs[7] and in cats[10]. A genetic predisposition to MAC infections may exist in basset hounds, Siamese cats[10] and in schnauzers[7]. Eggers *et al.* [7] detected depletion of T and B lymphocytes in three miniature schnauzers with disseminated mycobacteriosis. Evidence suggesting or corroborating immunosuppression could not be confirmed in this dog. Nevertheless, another fact should be considered. This dog was the only infected animal in a house with three other animals. The dog lived permanently in the backyard with three other animals: a dog and two cats. One

cat died almost at the same time as this dog; however, it was diagnosed with pulmonary carcinoma. Frozen tissue of this cat was tested for Mycobacterium spp. and resulted negative. The dog and another cat were monitored during four months, and no abnormalities were detected. Feces of these animals were collected twice and tested by culture and PCR for Mycobacterium spp. and were negative.

The cause of progressive anemia was not well defined. Renal lesions were considered insufficient to interfere with erythropoietin and produce anemia. Intestinal lesions could impair nutrient absorption, and a possible effect on red blood cell production may occur. Nevertheless, dissemination of macrophages loaded with myriads of bacterial rods throughout bone marrow could determine myelophthisis. The bone marrow was not examined in this case, but its involvement and consequent anemia in schnauzers with disseminated mycobacteriosis have been described[14,15].

The gastrointestinal route of infection could be suspected because the lesions were predominant in the gastrointestinal organs and less intense in the respiratory tract. The source of infection was possibly drinking water, since the owner reported that, some weeks before the animal presented with signs of disease, he found wild bird feces in the dog's drinking water. The backyard had some trees and birds (especially sparrows). Wild birds (sparrows, crows, and pigeons) may act as reservoirs and can shed the infection to the environment 17. The bacteria can persist in the environment for many years, especially in the soil[5,6].

MAC is an opportunistic pathogen in immunocompromised humans[2]. The dog was in close contact with its owners, but they had no history of disease.

Contributing Institution:
Veterinary School Universidade Federal de Minas Gerais
www.vet.ufmg.br

JPC Diagnoses:
1. Liver: Hepatitis, granulomatous, chronic, multifocal to coalescing, severe, with numerous intracytoplasmic bacilli.
2. Spleen: Splenitis, granulomatous, chronic, diffuse, severe, with numerous intracytoplasmic bacilli.
3. Lymph node: Lymphadenitis, granulomatous, chronic, diffuse, severe, with numerous intracytoplasmic bacilli.
4. Liver, spleen: Extramedullary hematopoiesis, diffuse, mild to moderate.

JPC Comment:
All clinical presentations of mycobacteriosis are uncommon in dogs, and disseminated disease is even rarer[4]. An interesting feature of mycobacteriosis in both dogs and cats is an apparent breed predisposition. In dogs, miniature schnauzers, as in this case, and basset hounds are predisposed. In cats, reported predispositions include the Siamese, Somali, and Abyssinian breeds[4,20]. These breed associations suggest underlying genetic factors, likely involving genes that impair the host's ability to recognize and neutralize *Mycobacterium* species.

The miniature schnauzer has the best-characterized genetic defect. Miniature schnauzers at increased risk of mycobacteriosis frequently harbor a CARD9 deficiency caused by a mutation in the CARD9 gene[4, 19, 21]. CARD9 is an adapter signaling protein best known for its critical role in antifungal immunity. Interestingly, humans with analogous CARD9 deficiencies do not appear predisposed to mycobacterial infections; however, as expected, they face a heightened risk of severe fungal

disease[21]. Notably, these patients often develop localized or systemic *Candida infections without* other predisposing conditions, a presentation characteristic of CARD9 deficiency[19]. Mechanistically, fungi are recognized by various pattern recognition receptors (PRRs), which recruit CARD9 to trigger the host innate immune response[21]. Although the presentation differs between humans and dogs, absent or minimal activation of the host's innate immune system against organisms that are generally nonpathogenic in healthy, immunocompetent individuals is a key unifying feature.

References:

1. Bauer N, Burkhardt S, Kirsch A, Weiss R, Moritz A, Baumgaertner W. Lymphadenopathy and diarrhea in a Miniature Schnauzer. *Vet Clin Pathol*. 2002;31:61-64.
2. Biet F, Boschiroli ML, Thorel MF, Guilloteau LA. Zoonotic aspects of *Mycobacterium bovis* and *Mycobacterium avium-intracellulare* complex (MAC). *Vet Res*. 2005;*36*:411-436.
3. Campora L, Corazza M, Zullino C, Ebani VV, Abramo F. *Mycobacterium avium* subspecies *hominissuis* disseminated infection in a Basset Hound dog. *J Vet Diagn Invest*. 2011;23:1083-1087.
4. Caswell JL, Willians KJ. Respiratory system. In: Jubb, Kennedy & Palmer's Pathology of Domestic Animals, ed. Maxie MG, 5th ed., Toronto, Canada: Elsevier Saunders; 2007:524-650.
5. Del Pilar Silva A, Leon CI, Guerrero MI, Neira R, Arias L, Rodriguez G. Avian tuberculosis of zoonotic importance at a zoo on the Bogotá Andean plateau (Sabana), Colombia. *Can Vet J.* 2009;50:841-845.
6. Dhama K, Mahendran M, Tiwari R, Dayal S, Kumar D, Sawant PM.
7. Tuberculosis in Birds: Insights into the *Mycobacterium avium* Infections. *Vet Med Int*. 2011. 2011: 712369.
8. Eggers JS, Parker GA, Braaf HA, Mense MG. Disseminated *Mycobacterium avium* infection in three Miniature Schnauzer littermates. J Vet Diagn Invest. 1997;9:424-427.
9. Quesada-Canales O, Díaz-Delgado J, Paz Y, Domínguez L, Bezos J, Calabuig P, et al. Disseminated avian mycobacteriosis in a free-living grey heron (*Ardea cinerea*). *Avian Dis*. 2013;57:703-706.
10. Haist V, Seehusen F, Moser I, Hotzel H, Deschl U, Baumgärtner W, et al. *Mycobacterium avium* subsp. *hominissuis* infection in 2 pet dogs, Germany. *Emerg Infect Dis*. 2008;14:988-990.
11. Jordan HL, Cohn LA, Armstrong PJ. Disseminated *Mycobacterium avium* complex infection in three Siamese cats. *J Am Vet Med Assoc*. 1994;204:90-93,
12. Kriz P, Kaevska M, Bartejsova I, Pavlik I. Mycobacterium avium subsp. avium found in raptors exposed to infected domestic fowl. *Avian Dis*. 2013;57:688-692.
13. Manarolla G, Liandris E, Pisoni G, Sassera D, Grilli G, Gallazzi D, et al. Avian mycobacteriosis in companion birds: 20-year survey. *Vet Microbiol.* 2009;133:323-327.
14. Martinho APV, Franco MMJ, Ribeiro MG, Perrotti IBM, Mangia SH, et al. Case Report: Disseminated *Mycobacterium tuberculosis* infection in a dog. *Am J Trop Med Hyg*. 2013; 88:596-600.

15. Miller MA, Greene CE, Brix AE. Disseminated *Mycobacterium avium-intracellulare* complex infection in a miniature schnauzer. *J Am Anim Hosp Assoc*. 1995;31:213-216.
16. O'Toole D, Tharp S, Thomsen BV, Tan E, Payeur JB. Fatal mycobacteriosis with hepatosplenomegaly in a young dog due to *Mycobacterium avium*. *J Vet Diagn Invest*. 2005;17:200-204.
17. Rindi L, Garzelli C. Genetic diversity and phylogeny of *Mycobacterium avium*. Infect Genet Evol. 2014;21:375-383.
18. Tell LA, Woods L, Cromie RL. Avian tuberculosis in birds, Review Science and Technology. *Office Internationale des Epizooties*. 2001;20: 180-203.
19. Ghielmetti G, Giger U. Mycobacterium avium: an Emerging Pathogen for Dog Breeds with Hereditary Immunodeficiencies. *Curr Clin Microbiol Rep*. 2020;7(3):67-80.
20. Sykes JE. Cutaneous Mycobacterioses of Cats and Dogs. *Vet Clin North Am Small Anim Pract.* 2025;55(2):237-249.
21. Drummond RA, Franco LM, Lionakis MS. Human CARD9: A Critical Molecule of Fungal Immune Surveillance. *Front Immunol*. 2018;9:1836.

CASE II:

Signalment:
8 years 3.5 months, Female, Slender-tailed Meerkat, *Suricata suricatta*

History:
An adult female meerkat housed in a zoological collection was found collapsed. Nine months previously, the animal had a 'fit' witnessed by the keepers, followed by a 'vacant' episode the following month. Skull radiographs during a routine health check two months later revealed a mild opacity in the region of the left caudal cerebrum. On the day of presentation, additional radiographs showed similar irregular soft-tissue densities in the same region. Due to the clinical suspicion of the cause of the neurological signs, anesthesia was not reversed, and an intracardiac barbiturate injection euthanized the animal. Additional findings included evidence of previous conspecific aggression, with crusting present over the ear pinna and distal tail.

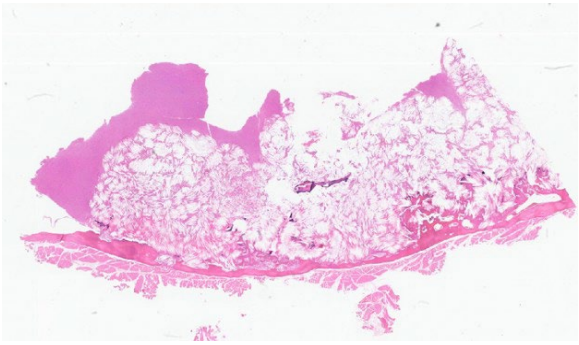

2-1. Brain and skull, slender-tailed meerkat (*Suricata suricatta*). Effacing a focally extensive region of brain parenchyma and eroding overlying bone are abundant negatively staining acicular clefts. (HE, 2x)

Gross Pathology:
Gross examination revealed a moderately thickened calvarium, with strong adhesions to the underlying, moderately thinned and friable cerebrum, with a moderate hydrocephalus.

Laboratory Results:
Serum cholesterol measured approximately 24 months and six months before euthanasia was 16.96 mmol/L and 13.01 mmol/L, respectively (ZIMS global species RI: 4.95-18.52 mmol/L).

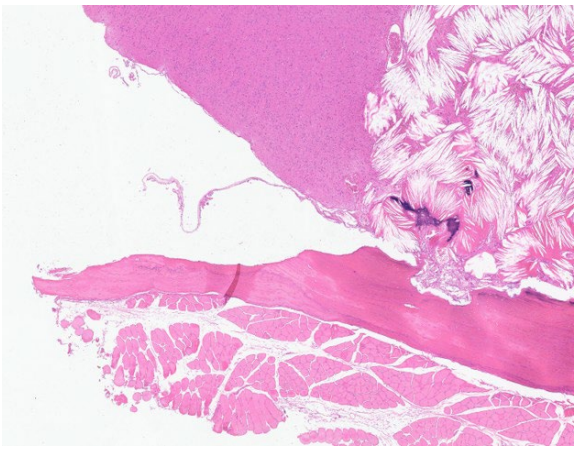

2-2. Brain and skull, slender-tailed meerkat (*Suricata suricatta*). Acicular clefts and inflammatory cells efface the gray matter and multifocally erode bone. (HE, 4x).

Microscopic Description:

Parietal skull with brain. Two sections of the cerebrum and overlying calvarium are examined; both are histologically similar. Occupying at least 75% of the sections, this focally extensive, poorly demarcated, irregularly shaped area expands the meninges and invades and replaces the cerebrum and calvarium. This area is composed of irregularly arranged clear elongate acicular cholesterol clefts. Between aggregates of these cholesterol clefts are variable amounts of cerebral parenchyma multifocally infiltrated by a moderate number of foamy haemosiderin-laden macrophages (haemosiderophages) and occasional lymphocytes and plasma cells. Within the cholesterol clefts and associated cerebral parenchyma are variably sized areas of hemorrhage. The cerebral parenchyma contains multifocal foci of mineralization, measuring up to 0.07mm in diameter. Adjacent to cholesterol clefts replacing the calvarium are low to moderate numbers of osteoclasts associated with areas of immature woven bone (bone remodeling).

Contributor's Morphologic Diagnoses:

1. Cerebrum, meninges, calvarium; focally extensive severe cholesterol granuloma with haemosiderophages and foci of mineralization
2. Calvarium; multifocal moderate bone remodeling

Contributor's Comment:

Cholesterol granulomas (cholesteatomas) are non-neoplastic, often asymptomatic, slow-growing aggregates of cholesterol crystals and macrophages within tissues.[8] They are most often diagnosed in older horses and are rarely found in other veterinary species, including dogs, cats, and, as in this case, meerkats.[1,3,5,6,8,9] In horses, cholesterol granulomas are benign masses associated with inflammation of the choroid plexus in the base of the lateral ventricles. They are often incidental findings on computed tomography (CT) scans or post-mortem examination. In horses, the

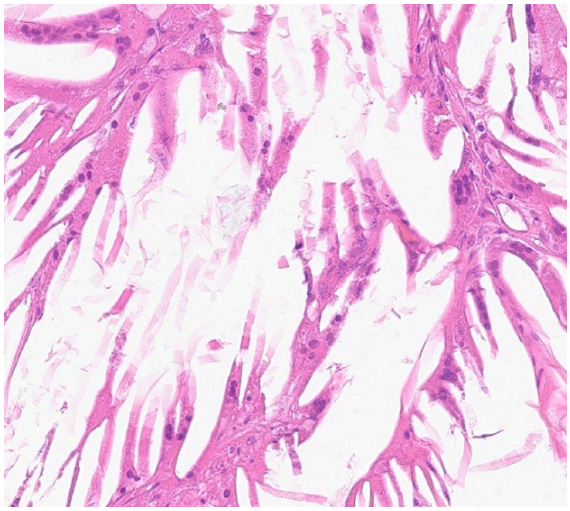

2-3. Brain, slender-tailed meerkat (*Suricata suricatta*). The cholesterol granuloma is composed of acicular clear clefts, macrophages with vacuolated cytoplasm, and multinucleated giant cells. (HE, 20x).

pathogenesis is thought to result from recurrent choroid plexus congestion, edema, and hemorrhage with degenerate erythrocytes, leading to cholesterol crystal formation and a foreign body-type response.[2] In humans, intracranial cholesterol granulomas have been associated with chronic middle ear disease and rarely disruption of nasal ventilation and drainage[7]. The exact pathogenesis is unclear but is believed to be like that in horses. In previous reports of cholesterol granulomas in meerkats, an association between chronic inflammation, hemorrhage and cholesterol crystal deposition has not been proven.[8] In this case, the small areas of hemorrhage and aggregates of haemosiderophages within the cholesterol granuloma may support a similar pathogenesis to that described in other species and question the role of trauma as the inciting cause. Conversely, the hemorrhage and inflammation could be secondary to the severe destruction of brain tissue and parietal bone.
Previous reports of cholesterol granulomas in meerkats describe them as originating from the meninges, with subsequent invasion into the cerebrum and overlying calvarium.[1,8] In this case, the severity of the destruction of brain tissue and bone hinders the diagnosis of the tissue of origin, but the invasion into both the brain and skull makes meningeal origin highly likely. Cholesterol granulomas in meerkats have also been found within the pericardium, renal cortex, pancreas, mesenteric lymph node, and spleen.[1,8]

In meerkats, neurological signs often preceded the diagnosis of a meningeal cholesterol granuloma and are believed to be associated with neuroparenchymal compression or destruction and obstruction of cerebrospinal fluid outflow.[1,8] In this case, there was no evidence of compression of the remaining cerebrum; however, the grossly observed hydrocephalus was

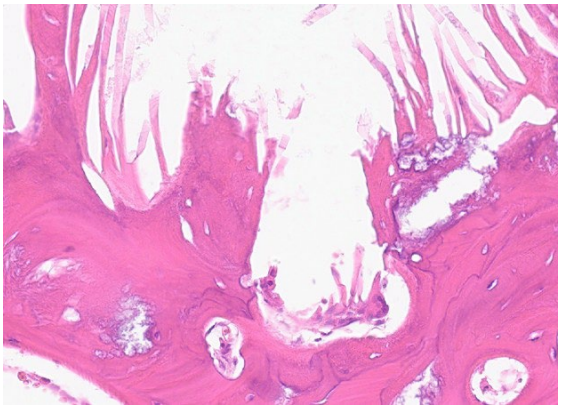

2-4. Skull, slender-tailed meerkat (*Suricata suricatta*). Areas of bone resorption adjacent to cholesterol clefts. There are multinucleated giant cells in resorption bays and scalloped, basophilic reversal lines. (HE, 10x)

likely due to the obstructed flow of cerebrospinal fluid secondary to the primary pathology. In reported cases of cholesterol granulomas in meerkats, serum cholesterol levels were elevated compared with captive and wild reference ranges.[1,8] Further supporting the hypothesis that elevated serum cholesterol may be associated with cholesterol cleft deposition, the captivity reference range for serum cholesterol in meerkats is suspected to be falsely elevated due to widespread hypercholesterolemia in zoological collections.[4] This highlights the importance of measuring serum cholesterol in meerkats exhibiting neurological signs and the need for reconsideration of the reference ranges. The underlying cause of hypercholesterolemia in captive meerkats is unknown and may represent a combination of factors, including diet, inborn errors in lipid metabolism and species-specific physiology.[8]

In this zoological collection, the meerkat diet consists of 'Hills Science Plan Feline Senior 7+ biscuits', a vegetable mix, and black crickets, with a no-mealworm policy due to their high saturated fat content.[4.] The decrease in this individual's serum cholesterol level from

16.96 mmol/L (655.8 mg/dL) to 13.01 mmol/L (503.1 mg/dL) 18 months later is believed to be due to a complete reduction in improper feeding by the general public. At the same time, the zoo was closed during the first few months of the Covid-19 lockdowns.

Preventing, diagnosing, and treating cholesterol granulomas in meerkats requires multidepartmental collaboration. Observing conspecific aggression by animal care staff offers the first opportunity to reduce trauma and address the suspected pathogenesis of cholesterol granulomas in meerkats. Next, veterinary investigation of neurological signs, including advanced diagnostic imaging and serum cholesterol monitoring, is the next step toward a clinical diagnosis. If done promptly, an on-site nutritionist can help achieve successful treatment. Lastly, post-mortem diagnosis of cholesterol granulomas supports clinical suspicion and helps gauge the effectiveness of current treatment protocols and dietary management. Cholesterol granulomas are a relatively common fatal disease in captive-bred meerkats, warranting further research into their pathogenesis to support the welfare of this common, zoologically housed exotic species.

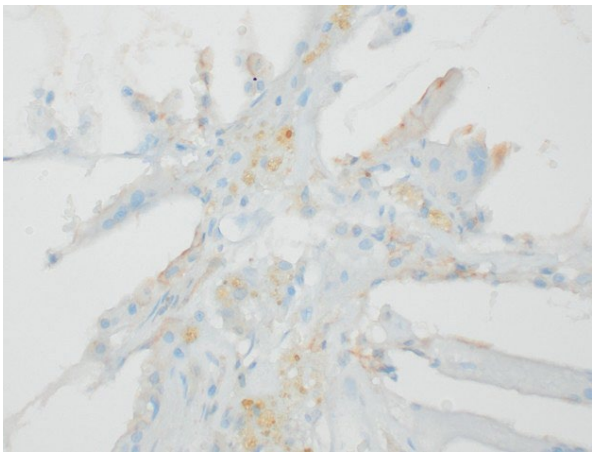

2-5. Brain, slender-tailed meerkat (*Suricata suricatta*). Macrophages and multinucleated giant cells have weak, cytoplasmic immunoreactivity to IBA-1. (IBA-1, 40x).

Contributing Institution:
Royal Veterinary College,
University of London
https://www.rvc.ac.uk/pathology-and-diagnostic-laboratories

JPC Diagnoses: Calvarium, meninges, cerebral gray matter: Cholesterol granuloma with calvarial osteolysis.

JPC Comment:
The contributor provided an excellent and thorough summary of cholesterol granulomas in both meerkats and domestic veterinary species. A notable feature of this case, consistent with previous meerkat reports, is the lesion's anatomic location and the substantial destruction of surrounding tissue relative to equine counterparts[1,8]. To date, five CNS cholesterol granulomas have been described in meerkats; all CNS-involved cases are located within the meninges. Destruction of the underlying gray matter and adjacent calvarium is gradual, with only minimal inflammatory reaction in the gray matter adjacent to the slowly expanding lesion[1,8].

As expected, the inflammatory cells exhibited diffuse cytoplasmic IBA1 immunoreactivity, confirming their identity as macrophages and macrophage-derived multinucleated giant cells. However, the macrophage cytoplasm was also brightly PAS-positive. This finding is interesting because pure lipids do not stain with PAS and are more reliably demonstrated using Oil Red O or Sudan Black B on frozen sections. Because PAS primarily stains carbohydrates and mucosubstances (glycoproteins), there are two potential mechanisms explaining this brilliant cytoplasmic PAS reactivity[11].

This intense positivity most likely reflects accumulated glycolipids, lipofuscin deposition, or a combination of both. Lipofuscin is a membrane-bound, insoluble wear-and-tear pigment containing carbohydrate and protein moieties that impart variable PAS positivity. Finally, while cholesterol processing is complex and cholesterol is predominantly stored in macrophages as cholesterol esters or lipoproteins, in environments of cholesterol saturation and poor drainage, lipid is likely also stored as glycolipids, which would be intensely PAS-positive[10].

References:

1. Allan KJ, Waters M, Ashton DG, Patterson-Kane JC. Meningeal cholesterol granulomas in two meerkats (Suricata suricatta). *Vet Rec*. 2006;**158**:636-637.
2. Cantile C, Youssef S. *Nervous System*. In: Maxie M. G. Jubb, Kennedy and Palmer's Pathology of Domestic Animals, 6th ed; 1: 304.
3. Davis AM, Lahmers K, Trusiano B, Zimmerman K, Romeiser J, Tuohy J. Cholesterol Granuloma of the Cranial Mediastinum in a Dog. *J Am Anim Hosp Assoc*. 2022;**58**:129-136.
4. Dobbs P, Liptovszky M, Moittie S. Dietary management of hypercholesterolemia in a bachelor group of zoo-housed slender-tailed meerkats Suricata suricatta. *J Zoo Aquar Res*. 2020;**8**:294-296.
5. Fliegner RA, Jubb KVF, Lording PM. Cholesterol Granuloma Associated with Otitis Media and Destruction of the Tympanic Bulla in a Dog. *Vet Pathol.* 2007;**44**:547-549.
6. Greci V, Travetti O, Di Giancamillo M, et al. Middle ear cholesteatoma in 11 dogs. *Can Vet J*. 2011;**52**:631-636.
7. Leon ME, Chavez C, Fyfe B, Nagorsky MJ, Garcia FU. Cholesterol granuloma of the maxillary sinus. *Arch Pathol Lab Med.* 2002;**126**:217-219.
8. Sladky KK, Dalldorf FG, Steinberg H, Wright JF, Loomis MR. Cholesterol granulomas in three meerkats (Suricata suricatta). *Vet Pathol.* 2000;**37**:684-686.
9. Van der Heyden S, Butaye P, Roels S. Cholesterol granuloma associated with otitis media and leptomeningitis in a cat due to a Streptococcus canis infection. *Can Vet J*. 2013;54:72-73.
10. Chistiakov DA, Bobryshev YV, Orekhov AN. Macrophage-mediated cholesterol handling in atherosclerosis. *J Cell Mol Med*. 2016;20(1):17-28.
11. Pernick N. Stains (IHC & specials) Mucins. PathologyOutlines.com, Inc. June 1, 2025. Accessed September 2, 2026. https://www.pathologyoutlines.com/topic/stainsmucins.html

CASE III:

Signalment:
A ten-year-old castrated male domestic shorthaired cat.

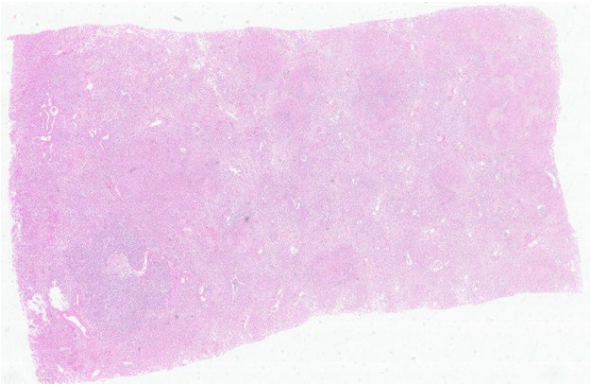

3-1. Liver, cat. One section of liver is submitted. The liver has a focal region of tubular proliferation and multifocal to coalescing areas of pallor.

History:
The cat had relapsing icterus, anemia, and lethargy following an episode of similar clinical signs 2 months before presentation. The cat was treated with conservative care and showed minor improvement; its owners elected euthanasia.

Gross Pathology:
Pale and yellow mucous membranes and severe flea infestation. A small amount of transparent pericardial fluid was noted. The liver is diffusely yellow, has an irregular, rugged surface with multifocal nodules, and a single 2-centimeter, slightly firm, roughly spherical mass in the right central lobe. The adrenal glands are bilaterally symmetrically enlarged. The mesenteric lymph nodes are moderately enlarged but retain normal architecture.

Laboratory Results:
Titer of 1:1024 for antibodies to Toxoplasma *gondii*

Microscopic Description:
Liver: The liver is expanded by a well-demarcated, unencapsulated, expansile, moderately dense cellular neoplastic cell proliferation. The neoplastic cells are arranged as closely packed tubules and are supported by small amounts of fibrous stroma. The neoplastic cells are cuboidal to polygonal, have variably distinct cell borders, and small to moderate amounts of eosinophilic cytoplasm. The nuclei are intermediate to large, centrally located, have finely stippled chromatin, and 1-2 inconspicuous nucleoli. Anisokaryosis and anisocytosis are mild to moderate. Mitotic index is 10. Within the neoplastic cell proliferation and the adjacent liver, there are multiple randomly distributed foci of coagulative necrosis, admixed with small numbers of neutrophils, macrophages, lymphocytes, and plasma cells (most prominent at the periphery of the necrotic foci). Within the necrotic foci, there are numerous 20-30 micrometer in diameter, round to oval parasitic cysts; each one has a thin 0.5 micrometer basophilic cyst wall and contains numerous 2-3 micrometer, basophilic round to banana-shaped bradyzoites. Occasionally, scattered tachyzoites are present within macrophages and hepatocytes.

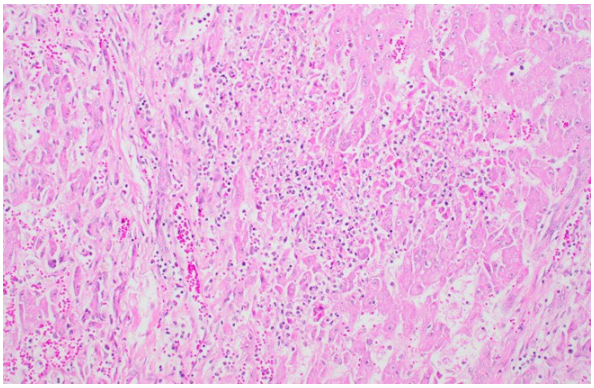

3-2. Liver, cat. There are multifocal to coalescing areas of lytic necrosis and hemorrhage with adjacent degenerating and necrotic hepatocytes.

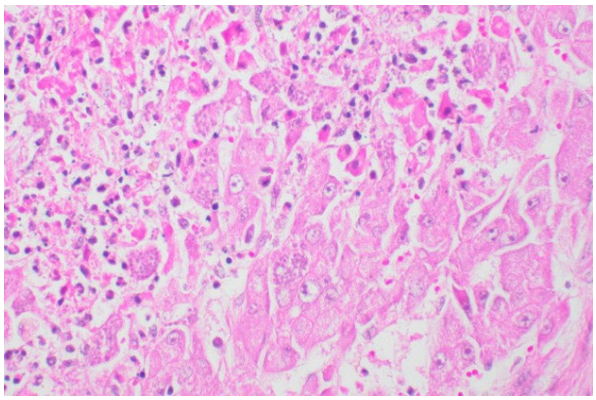

3-3. Liver, cat. At the periphery of areas of necrosis there are many intracytoplasmic and extracellular apicomplexan zoites. Zoites are within the cytoplasm of both hepatocytes and macrophages. (HE, 40x).

Contributor's Morphologic Diagnoses:
Liver:
1) Cholangioma.

2) Severe, multifocal to coalescing acute necrotizing hepatitis with myriad protozoal cysts and zoites (consistent with *Toxoplasma).*

Contributor's Comment:
Lesions in other organs include severe necrotizing adrenalitis with protozoal cysts, mild lymphocytic myocarditis, and mild interstitial pneumonia with pulmonary edema. Immunohistochemistry for *Toxoplasma gondii* showed strong positive staining.

Toxoplasma gondii uses felids as definitive hosts and is heteroxenous - cats can be infected by ingesting asexual stages in prey tissue or by ingesting oocysts. In intermediate hosts and in cats, asexual development occurs in many organs and tissues.

Toxoplasma gondii (and Neospora caninum) are unique among protists because of their ability to parasitize a wide range of hosts. Natural infection occurs in birds, primates (including humans), rodents, insectivores, herbivores, and carnivores. Systemic toxoplasmosis occurs most often in immunologically immature or immunocompromised animals. In the cat, intestinal and systemic infection occur almost simultaneously. It can spread via lymphocytes to the lymph nodes and from there to the blood/lymph and portal circulation to the liver.

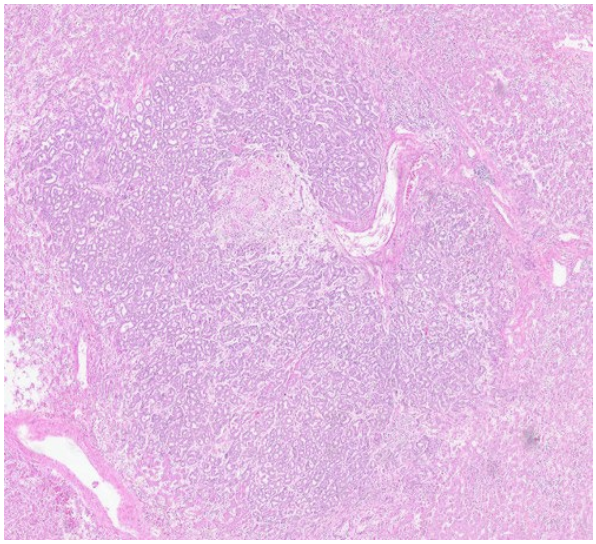

3-4. Liver, cat. There is a focal, unencapsulated, well demarcated neoplasm composed predominantly of irregular tubules. (HE, 2x).

Focal necrosis is common and appears to be related to rapid replication of tachyzoites. Immune animals develop a chronic or dormant form of toxoplasma infection that is characterized by the formation of cysts containing bradyzoites. In the liver, irregular foci of coagulative necrosis are scattered randomly; usually, only little inflammation is associated with the necrotic area. variable number of tachyzoites may be present in hepatocytes and Kupffer cells, usually at the periphery of the lesions. In the adrenals, vast areas of necrosis are usually seen in the adrenal cortex with minimal inflammation.

The hepatic neoplasm in this case is an incidental finding. We discuss three differentials. diagnoses for it. Cholangiocarcinoma, biliary cystadenoma (the proper term now is congenital biliary cysts), and cholangioma. The small size, demarcation, low cellular pleomorphism, lack of invasion or metastases, lack of substantial desmoplasia, and lack of aggregates of hepatocytes between the neoplastic tubules favored the diagnosis of cholangioma.

Contributing Institution:
Kimron Veterinary Institute
https://www.gov.il/en/government-service-branches/veterinary_institute

JPC Diagnoses:
1. Liver: Hepatitis, necrotizing, subacute, multifocal to coalescing, marked, with intrahepatocytic, intra-histiocytic, and extracellular apicomplexan zoites.

2. Liver: Biliary adenoma.

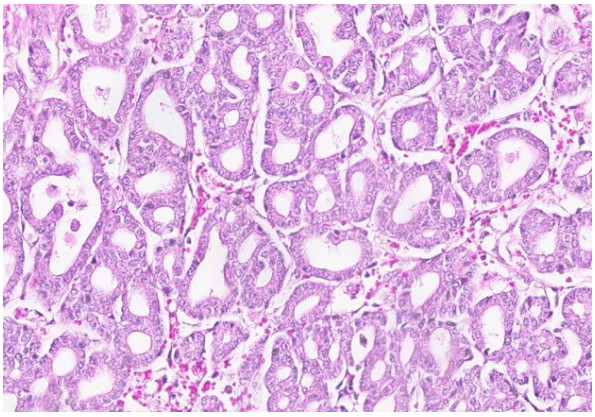

3-5. Liver, cat. The neoplastic tubules are composed of cuboidal epithelial cells that have distinct cell borders, a high N:C ratio and scant cytoplasm, and a round nucleus with vesiculate chromatin and 1-2 distinct nucleoli. Mitotic figures are rare. (HE, 30x).

JPC Comment:

Conference discussion for this case focused on differentiating biliary hyperplasia, biliary adenoma, and cholangiocarcinoma, as well as the differential diagnoses for feline hepatic necrosis. In the primary liver section evaluated by WSC staff and the conference moderator, the proliferation of irregular bile ducts was predominantly focal, featuring several satellite lobules adjacent to the main lesion. In subsequent sections cut for the resident unknown slide, special stains, and immunohistochemistry, the proliferative mass was diminished in extent, appearing as a single, 3-mm-diameter lobule of relatively well-differentiated bile ducts. For this reason, the presenting resident favored biliary hyperplasia, aligning with her top differential diagnosis for the concurrent hepatic necrosis, which was acetaminophen toxicosis. Although hepatic necrosis, bile duct proliferation, and cholestasis are recognized findings in feline acetaminophen toxicity, three primary features rule out that diagnosis in this case[1].

First, although extensive necrosis obscures the architectural pattern, several centrilobular and periportal regions remain unaffected. These spared regions support a multifocal to coalescing, random pattern of necrosis, which is inconsistent with hepatotoxins like acetaminophen that classically cause centrilobular to midzonal necrosis.

Second, the necrotic foci are directly centered on intra- and extracellular apicomplexan zoites. Felids serve as both the definitive and intermediate hosts for *Toxoplasma gondii*[1]. In intermediate hosts, primary infection typically transitions to subclinical, chronic carriage of dormant tissue cysts. However, immunosuppression or concurrent disease impairs the CD8+ T-cell and interferon-gamma responses that maintain encystment, which precipitates rupture of tissue cysts and clinical disease[4]. Although a predisposing cause of immunosuppression was not definitive in this animal's clinical history, common triggers include young age or concurrent immunosuppressive viral infections (e.g., feline leukemia virus, feline immunodeficiency virus, or feline panleukopenia virus)[5,6].

Finally, while ductular reaction occurs in subacute feline acetaminophen hepatopathy, marked, solitary focal proliferation is atypical. Acetaminophen-induced ductular change typically presents as a diffuse or multifocal periportal increase in bile duct profiles rather than a discrete focal nodule.

References:

1. Jubb, Kennedy and Palmer's Pathology of Domestic Animals Fifth edition vol I p437, vol 2 p270-272, vol 3 p410
2. Stacey A. Elmore, Jeffrey L. Jones, Patricia A. Conrad, Sharon Patton, David S. Lindsay, and J.P. Dubay. Toxoplasma

gondii: epidemiology, feline clinical aspects, and prevention. 2010.

3. Donald J. Meuten. Tumors in domestic animals. 2002;9:493-498
4. Durieux MF, Lopez JG, Banjari M, et al. Toxoplasmosis in patients with an autoimmune disease and immunosuppressive agents: A multicenter study and literature review. *PLoS Negl Trop Dis*. 2022;16(8):e0010691.
5. Moore A, Burrows AK, Malik R, Ghubash RM, Last RD, Remaj B. Fatal disseminated toxoplasmosis in a feline immunodeficiency virus-positive cat receiving oclacitinib for feline atopic skin syndrome. *Vet Dermatol.* 2022;33(5):435-439.
6. Bártová E, Sedlák K, Vodlan Š, Budíková M, Račka K. Seroprevalence of Toxoplasma gondii and Feline Immunodeficiency Virus in Domestic Cats and Their Associations with Clinical Signs. *Acta Parasitol.* 2026;71(4):149.

CASE IV:

Signalment:
9-year-old, spayed female, Labrador mixed breed dog (*Canis lupus familiaris)*

History: The dog developed non-pruritic periocular and dorsal trunk crusting and alopecia approximately 6 weeks prior. A skin scrape of the affected skin was negative. The dog was treated with Cytopoint, Bravecto, and a two week course of Clavamox. Over the next two weeks, the alopecia and crusting spread around her eyes and down to the nose. Periocular areas were treated with topical neo/poly/dex eye
ointment. On recheck, the skin around the nasal mucosa and lips was depigmented, with evidence of uveitis.

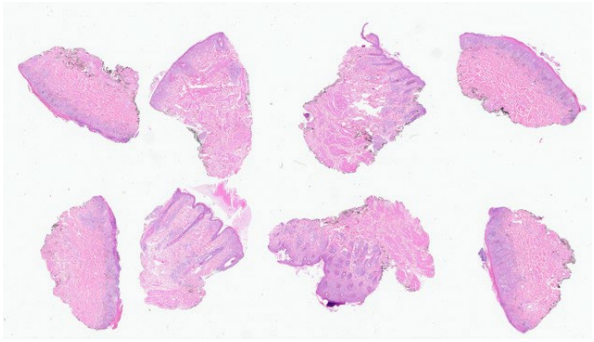

4-1. Haired skin and mucosa, dog. Eight sections of haired skin and mucosa from the face and lips of a dog were submitted for consideration. From subgross there is a lichenoid cellular infiltrate in all sections and multiple sections have erosion of the overlying epithelium. (HE, 1x).

Gross Pathology:
Five punch biopsies of the affected skin around the nose and lip are submitted for histopathology. The epidermal surface of the biopsies is multifocally ulcerated, mottled tan to black, and contains sparse hair. A soft to firm, approximately 2.5 cm subcutaneous mass from the left cranial thorax is submitted alongside the punch biopsies.

Laboratory Results:
Skin culture: *Staphylococcus* spp.

Microscopic Description:
Facial skin (mucocutaneous junction, haired skin, and lips). The mucosal, submucosal, and dermal-epidermal interface is infiltrated by a marked inflammatory infiltrate consisting of macrophages and neutrophils with fewer lymphocytes and plasma cells. Similar inflammation is present in periadnexal areas and occasionally perivascularly. Macrophages containing fine to large, dark brown, cytoplasmic pigment (melanophages) infiltrate the superficial submucosa and are scattered along areas of inflammation (pigmentary incontinence). Rete

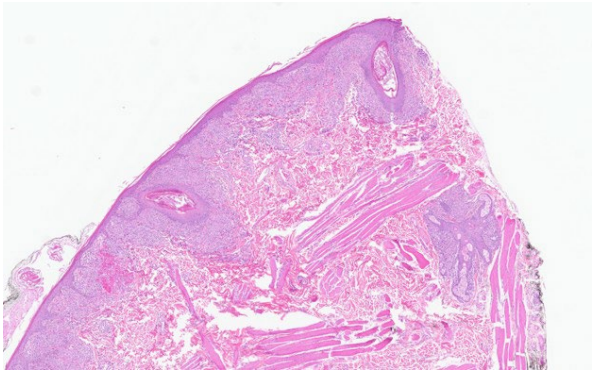

4-2. Lip, mucocutaneous junction, dog. There is a superficial lichenoid, perifollicular, and periadnexal band of inflammation with multifocal hemorrhage. (HE, 2x)

pegs multifocally extend into the superficial mucosa (mucosal hyperplasia), and the mucosal surface is covered in a moderate amount of nucleated keratin (parakeratotic hyperkeratosis). The superficial mucosal surface is multifocally ulcerated and replaced by serocellular crust composed of degenerate neutrophils and karyorrhectic cellular debris mixed with occasional colonies of basophilic cocci. The epidermal surface is covered in a moderate amount of anucleate keratin (orthokeratotic hyperkeratosis).

Other histopathology findings that are not included in the provided slide:

Left cranial thorax: Soft Tissue Sarcoma (Grade 2, Medium Grade)

Contributor's Morphologic Diagnoses:

1. Facial skin: Pyogranulomatous lichenoid dermatitis with pigmentary incontinence

Contributor's Comment:

The histopathological features of the facial skin and clinical history are compatible with uveodermatologic syndrome (UDS). Uveodermatologic syndrome is a rare, suspected immune-mediated skin disease characterized by granulomatous uveitis and facial depigmentation.[3] In humans, a similar disease entity, "Vogt-Koyanagi-Harada," results in comparable skin lesions in addition to meningitis with occasional auditory involvement; neurological disease is exceptionally rare in dogs; thus, this disease is referred to as UDS instead of VKH in dogs.[1,6] The pathogenesis of VKH in humans demonstrates T cell-mediated autoimmunity against melanin and related proteins; however, this pathogenesis has not been demonstrated in the dog.[3] Numerous genetic mutations related to immunity and aberrant activation of Th1 and Th17 pathways have been discovered in humans who develop VKH.[8] Studies in Akitas with UDS suggest a role of certain dog leukocyte antigen (DLA) class II gene alleles in the pathogenesis of this disease,[1,4,6,7] which is similar to studies in humans that have found an association with human leukocyte antigen (HLA) class II alleles in the formation of VKH.[2]

Arctic breeds such as Siberian Huskies, Alaskan Malamutes, Akitas, Samoyeds, Chow Chows, and related mixed breed dogs are more commonly affected. This disease has

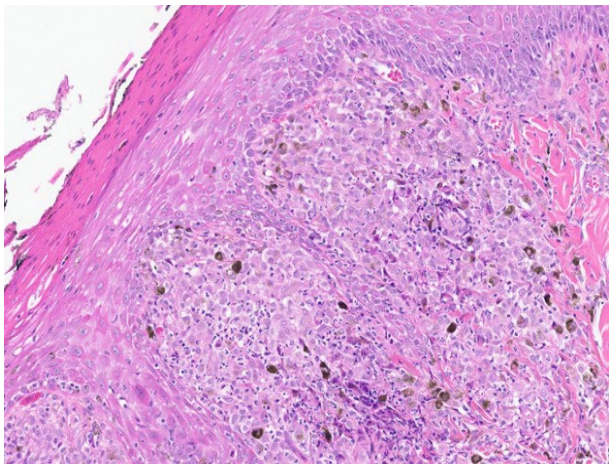

4-3. Mucosa, dog. The lichenoid band of inflammation is composed predominantly of macrophages and neutrophils. Macrophages frequently contain scant to abundant intracytoplasmic melanin. (HE, 20x)

also been diagnosed in the Irish setter, golden retriever, Old English sheepdog, Saint Bernard, Shetland sheepdog, Dachshund, fox terrier, Basset hound, Brazilian fila, Jack Russell terrier, rat terrier, and miniature poodle.[3,5,6] The most common ages affected are between 6 months and 6 years, and there is no known sex predilection.[3] Ocular signs include anterior and posterior uveitis that presents as photophobia, blepharospasm, conjunctivitis, and corneal edema.[3,6,7] Skin signs include bilaterally symmetric facial depigmentation with variable amounts of crusting and erythema, predominantly along the muzzle, periorbital region, nasal planum, and lips.[3,4] Lesions may also appear on the external genitalia including the scrotum and vulva, inside the oral cavity, or become more generalized throughout the body.[3,4] These lesions may or may not be pruritic. The ocular form of this disease often precedes skin lesions, and affected individuals may not have skin lesions at all; however, concurrent skin disease is an important indicator of the ocular form.[3,7]

Histologically, the epidermis is hyperplastic, with variable amounts of crusting, ulceration, parakeratosis, and leukocyte exocytosis.[3] Oftentimes, the stratum basale has decreased or absent melanin.[3] Basal cell degeneration is rare, which helps distinguish it from other immune-mediated causes of dermatitis such as

discoid lupus erythematosus.[3] There is perivascular to lichenoid dermatitis composed of predominantly large macrophages with fewer neutrophils, lymphocytes, and plasma cells that may extend to periadnexal areas.[3,4] Frequently, macrophages will contain fine "dust-like", granular or clumped melanin pigment signifying pigmentary incontinence.[3,4,6] Inflammation composed predominantly of macrophages with fine melanin pigment is another key feature in distinguishing this disease from discoid lupus erythematosus.[3,6] In chronic lesions, dermal inflammation may be mild.[3]

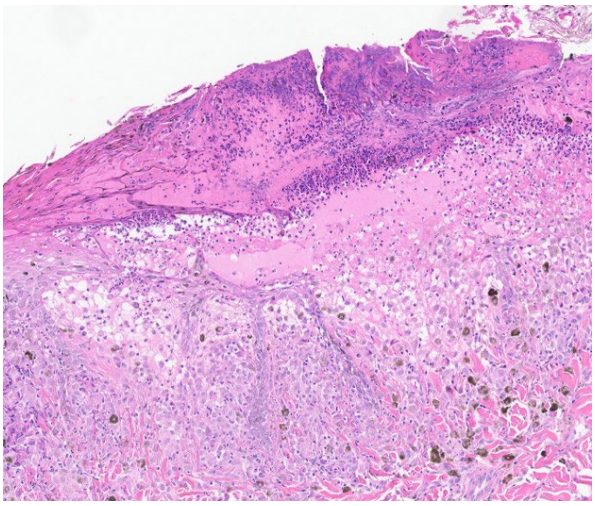

4-4. Haired skin, dog. There are multifocal ulcers with loss of the overlying epithelium and replacement by a serocellular crust, edema, hemorrhage, and neutrophilic inflammation. (HE, 10x)

The preferred sites of biopsy include areas of depigmentation, crusting, and erythema around the lips and dorsal muzzle.[3] It is best to avoid areas of trauma, as secondary infections may obscure important histopathologic lesions.[3] In this individual's case, infection was superficial and did not impact histopathologic diagnosis of UDS.

Contributing Institution:
University of Illinois at Urbana-Champaign, Veterinary Diagnostic Laboratory
https://vdl.vetmed.illinois.edu/

JPC Diagnoses:
1. Haired skin: Dermatitis, lichenoid, histiocytic, chronic, diffuse, marked with pigmentary incontinence.
2. Mucosal membrane: Mucositis, lichenoid, histiocytic, chronic, diffuse, marked with pigmentary incontinence.

JPC Comment:
In humans, autoantibodies against tyrosinase and related melanocytic proteins drive Vogt-

Koyanagi-Harada (VKH) syndrome. The tissue distribution of melanocytes accounts for its characteristic presentation of lesions across the uvea, skin, inner ear, and meninges. Canine uveodermatologic syndrome, the disease counterpart in dogs, shares this focus on tissues rich in native melanocytes; however, in dogs, the presentation is almost exclusively limited to ocular and dermatologic lesions. Notably, a recent case report described uveodermatologic syndrome in a dog presenting with ocular lesions and aseptic meningitis without cutaneous involvement. In that patient, the ocular lesions preceded the neurologic signs and became severe enough to require bilateral enucleation to preserve comfort.

During the conference, speakers noted that Akita appear to have a stronger predisposition for immune-mediated diseases than many other breeds. While purebred dogs generally carry a higher risk of inheriting genetic conditions due to selective breeding and occasional practices that neglect outbreeding or genetic testing, the American Akita faces an even greater risk. As the contributor described, this elevated susceptibility likely stems from a unique combination of DLA class II genes that have remained conserved within a small population with limited genetic diversity.

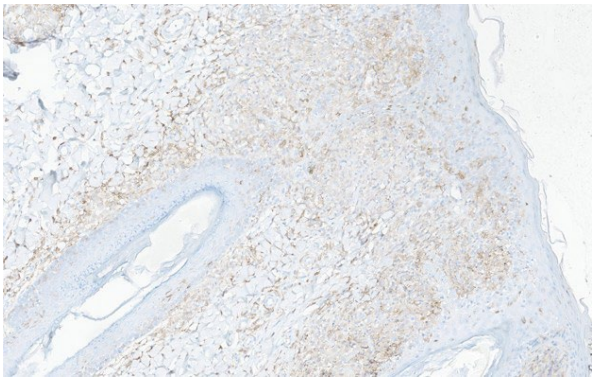

4-5. Haired skin, dog. The lichenoid and perifollicular dermatitis is composed of histiocytes that have diffuse, moderate, cytoplasmic IBA-1 immunoreactivity. (IBA-1, 15x)

The American Akita is a remarkable breed with historical roots in Japan. Early ancestors of the breed were smaller, close to the size of a fox, yet known for steadfast loyalty. This loyalty is best known through the true story of Hachikō, an Akita owned by a university professor. Each day, Hachikō met his owner at the train station after work. Following the professor's sudden death at the university, Hachikō continued returning to the station daily, waiting faithfully until his own death years later. Today, a bronze statue at the station honors his memory, and families across Japan continue to share his story as an enduring symbol of devotion. In the United States, Helen Keller owned one. The Japanese government gifted her a pair after she expressed deep admiration for Hachikō during a visit to Japan.

References:

1. Angles JM, Famula TR, Pedersen NC. Uveodermatologic (VKH-like) syndrome in American Akita dogs is associated with an increased frequency of DQAl *00201. Tissue Antigens. 2005; 66:656-665.
2. Anukul N et al. HLA-DRBl *04:05 and HLA-DQBl *04:01: Alleles potentially associated with Vogt-Koyanagi-Harada in Northern Thai Patients. Ocul Immunol Inflamm. 2021; 29(2):260-263.
3. Gross TL, Ihrke PJ, Walder EJ, et al. Lichenoid diseases of the dermis. In: Skin Diseases of the Dog and Cat. 2nd Edition. 9600 Garsington Road, Oxford OX4 2DQ, UK: Blackwell Science; 2005.
4. Hargis AM, Myers S. Integumentary system. In: Zachary JF, Pathologic Basis of Veterinary Disease. 6th ed. St. Louis, MO: Mosby Inc; 2016: 1104.
5. Kang MH, Lim CY, Park HM. Uveodermatologic syndrome concurrent with

keratoconjunctivitis sicca in a miniature poodle dog. Can Vet J. 2014;55(6):585-8.

6. Mauldin EA, Peters-Kennedy J. Integumentary system. In: Maxie MG, ed. *Jubb, Kennedy, and Palmer's Pathology of Domestic Animals.* Vol 2. 6th St. Louis, MO: Elsevier; 2016.
7. Zarfoss MZ, et al. Clinical findings and outcomes for dogs with uveodermatologic syndrome. J Am Vet Med Assoc. 2018; 252(10): 1263-1271.
8. Zhou C, et al. Genetic association of PRKCD and CARD9 polymorphisms with Vogt-Koyanagi-Harada disease in the Chinese Han population. Hum Genomics. 2023; 17(9):1-8.
5. Lam JPM, Rozsa B, Paulin MV, et al. Uveodermatologic syndrome presenting with concurrent aseptic meningoencephalitis in a dog. *Can Vet J*. 2025;66(2):130-137.
6. Yamaki K, Gocho K, Hayakawa K, Kondo I, Sakuragi S. Tyrosinase family proteins are antigens specific to Vogt-Koyanagi-Harada disease. *J Immunol.* 2000;165(12):7323-7329.
7. Flaim D. Akita History: Hachikō & the Revival of the Devoted Japanese Breed. American Kennel Club. September 20, 2023. Accessed September 2, 2026. https://www.akc.org/expert-advice/dog-breeds/akita-history-hachiko-japanese-breed/